Contemporary Engineering Sciences, Vol. 1, 2008, no. 3, 127 - 138

L-Band SiGe HBT Differential Amplifiers with Multiple Bandpass or Bandstop Performance Using Stacked Parallel-Resonant Circuits

Yasushi Itoh

1-1-25 Tsujido-Nishikaigan
Fujisawa, Kanagawa, 251-8511 Japan
itoh@elec.shonan-it.ac.jp

Abstract

L-band SiGe HBT differential amplifiers with multiple bandpass or bandstop performance is presented. It incorporates stacked parallel-resonant circuits into the design of the output load of the differential amplifier to achieve multiple bandpass performance. On the other hand, the stacked parallel-resonant circuits are used between emitters of the differential transistor-pair to achieve multiple bandstop performance. With the use of the stacked parallel-resonant circuits, the quad-band bandpass amplifier demonstrates an averages gain of 9 dB at 0.54, 0.7, 1.08, and 1.39 GHz. On the other hand, the quad-band bandstop amplifier shows an averaged bandstop level of 6 dB at 0.34, 0.56, 0.73, and 1.07 GHz. The multiple bandpass or bandstop technologies are considered to be one of the candidates supporting the next generation multiband, multimode, adaptive or reconfigurable wireless radios.

Keywords: microwave, amplifier, differential, multiband, multimode, SiGe HBT

1 Introduction

Recently, there is a growing need to develop multiband and multimode RF circuits for the next-generation wireless radios [1]. Under this background, a number of multiband amplifiers are aggressively researched and developed. The multiband amplifiers are categorized into two groups. The 1st group achieves a multiband performance by switching amplifiers, matching circuits, or bias [2].

The 2nd group employs a simultaneous matching technique [3]. A wideband matching is also included in the 2nd group [4]. The 1st group includes switched-off, non-operated amplifiers or matching circuits, leading to larger size or high power-consumption. A wideband matching of the 2nd group amplifies unwanted signals at the same time, leading to a serious interference problem. As a result, the simultaneous matching is considered to be the best choice in circuit performance. However, the circuit design is rather complicated and thus the number of matching bands is limited to only two (dual-band) [3].

On the other hand, with the rapid and increasing growth of wireless and mobile communication systems, the interference and image rejection of collocated active radios in both frequency and space become a crucial issue especially for the multiband and multimode applications [5]. To address this problem, the CMOS LNA with image rejection filters [6], [7] and the differential phase rotator [5] have been proposed as an active interference canceller. These active interference cancellers are not suitable from the viewpoint of the differential amplifier design as well as the multiband and multimode applications.

To overcome these problems, two types of the differential amplifiers with multiple bandpass or bandstop performance are proposed in this paper. The multiband bandpass amplifier incorporates stacked parallel-resonant circuits into the design of the output load of the differential amplifier to achieve multiple bandpass performance. On the other hand, the multiband bandstop amplifier employs stacked parallel-resonant circuits between emitters of the differential transistor-pair to achieve multiple bandstop performance. In this paper, the design, fabrication, and performance of the L-band differential amplifiers with quad-band bandpass or bandstop performance are presented.

2 Principles of Circuit Design

A basic circuit topology of the multiband bandpass or bandstop differential amplifiers is shown in Fig. 1. Z_L is load impedance. Z_S is source impedance connected between emitters of the differential transistor-pair. At relatively low frequencies, the gain of the differential amplifier can be represented as follows:

$$G_L = \left| \frac{Z_L}{Z_S} \right| \tag{1}$$

To increase the gain of Equation (1), it is required that Z_S becomes small or Z_L becomes large. A series LC circuit makes Z_S small and a parallel LC circuit makes Z_L large at a resonant frequency. A much steeper resonance can be obtained for the parallel LC circuit because of an abrupt variation of the impedance. On the other hand, to decrease the gain of Equation (1), it is required that Z_S becomes large or Z_L becomes small. A parallel LC circuit makes Z_S large and a series LC circuit makes Z_S small. As compared with the series LC circuit, the parallel LC

circuit shows a steeper resonance because of an abrupt variation of the impedance. As a result, the parallel LC circuit is chosen for both bandpass and bandstop amplifiers. In addition, to achieve multiple bandpass or bandstop performance, the parallel LC circuit is cascaded in a stacked configuration, as shown in Fig. 1. The stacked parallel-resonant circuits have an outstanding feature in that the resonant frequencies can be determined independently.

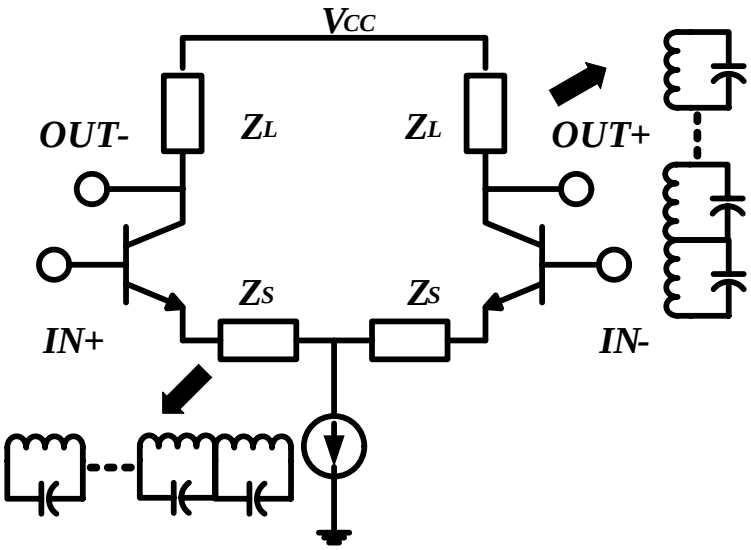

Fig. 1 Basic circuit topology of the multiband bandpass or bandstop differential amplifiers

3 Circuit Design

3.1 Quad-Band Bandpass Amplifier

A schematic diagram of the quad-band bandpass amplifier is shown in Fig. 2. The amplifier employs stacked parallel-resonant circuits for Z_L and a short circuit for Z_S. The stacked parallel-resonant circuits have a resonant frequency of f_1 and f_3 for the left-hand load, f_2 and f_4 for the right-hand load. The input matching circuit employs a lossy matching to achieve wide bandwidth including f_1, f_2, f_3 and f_4. The output signal from OUT- has a frequency of f_1 and f_3. On the other hand, the output signal from OUT+ has a frequency of f_2 and f_4.

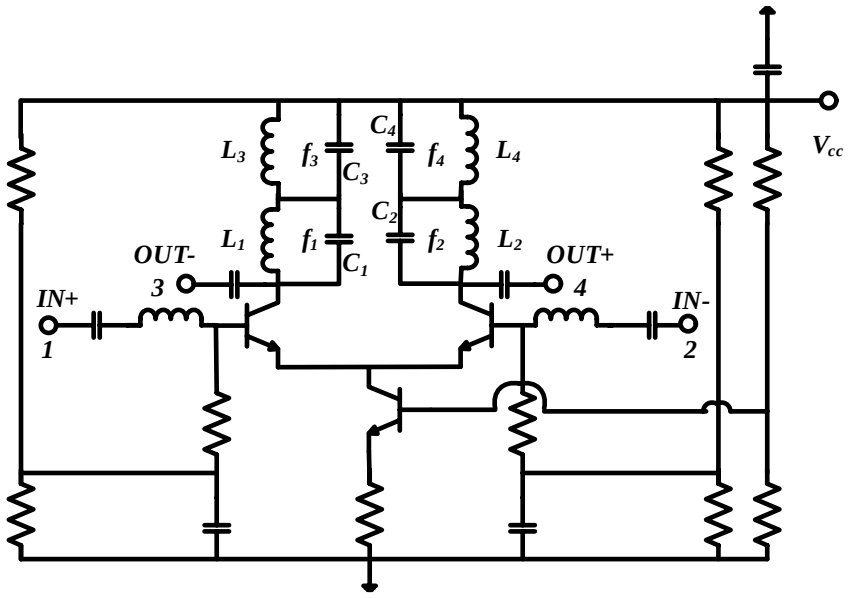

Fig. 2 Schematic diagram of the quad-band bandpass amplifier

The amplifier was designed so that f_1, f_2, f_3 and f_4 are 0.4, 0.8, 1.2, and 1.6 GHz, respectively. The resonant frequency can be obtained from the following equation.

$$f = \frac{1}{2\pi\sqrt{LC}} \tag{2}$$

The amplifier was designed to achieve a gain of greater than 10 dB and a return loss of better than 10 dB at f_1, f_2, f_3 and f_4. The simulated results are shown in Fig. 3. S_{11} and S_{22} are an input return loss. S_{33} and S_{44} are an output return loss. The port number is shown in Fig. 2. S_{41} and S_{32} are a forward gain. Since S_{31} and S_{42} were almost the same as S_{32} and S_{41}, these parameters are not shown in Fig. 3. Although the gain at f_1 is lower than that of f_2, f_3 or f_4, and the output return loss at f_4 is slightly less than 10 dB, multiple bandpass performance can be realized at f_1, f_2, f_3 and f_4. The circuit simulation was accomplished by using Agilent ADS. Bias condition is V_{cc} = 6 V, where V_{cc} is a supply voltage. In the simulation, 0.35 micron SiGe HBTs (Toshiba MT4S102T) with f_t = 25 GHz is used. The SPICE model (Gummel-Poon Model) is employed for linear and nonlinear calculations. The measured S-parameters are used for chip inductors, capacitors, and resistors consisting of the circuit. The simulated bandpass frequencies in Fig. 3 are slightly lower than the target frequencies of 0.4, 0.8, 1.2, and 1.6 GHz. This is mainly due to the fact that the chip inductors, capacitors, and resistors include parasitic elements.

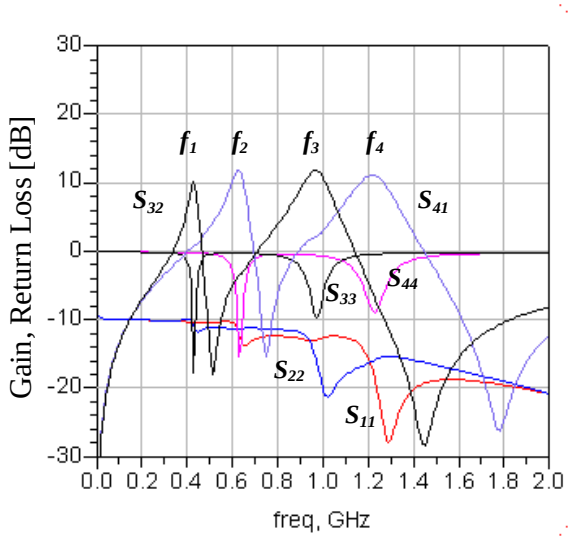

Fig. 3 Simulated results of the quad-band bandpass amplifier

3.2 Quad-Band Bandstop Amplifier

A schematic diagram of the quad-band bandstop amplifier is shown in Fig. 4. The amplifier employs stacked parallel-resonant circuits for Z_S and a series RL circuit for Z_L. The stacked parallel-resonant circuit has a resonant frequency of f_1, f_2, f_3 and f_4.

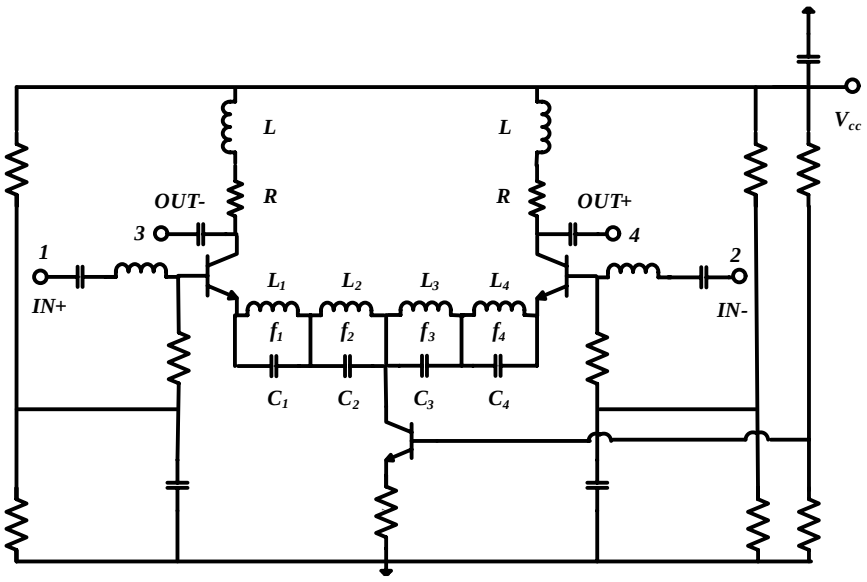

Fig. 4 Schematic diagram of the quad-band bandstop amplifier

The input matching circuit employs a lossy matching to achieve wide bandwidth including f_1, f_2, f_3 and f_4. The output signals having a bandstop frequency of f_1, f_2, f_3 and f_4 are delivered from OUT- and OUT+, respectively. The output signals from OUT- and OUT+ are out of phase.

The amplifier was designed so that f_1, f_2, f_3 and f_4 are 0.3, 0.5, 0.7, and 1 GHz, respectively. The resonant frequency can be obtained from Equation (2). The amplifier was designed to achieve a bandstop level of greater than 10 dB and a return loss of better than 10 dB at f_1, f_2, f_3 and f_4. The simulated results are shown in Fig. 5. S_{11} is an input return loss. S_{44} is an output return loss. S_{41} is a forward gain. The MSG/MAG is also shown in Fig. 5. Since the forward gains of S_{31}, S_{32}, and S_{42} were almost the same as S_{41}, these parameters are not shown in Fig. 5. In addition, since the return losses of S_{22} and S_{33} are almost the same as S_{11} and S_{44}, these parameters are not shown in Fig. 5. Although the bandstop level at f_1 is less than 10 dB, multiple bandstop performance can be realized at f_1, f_2, f_3 and f_4. The reason why the bandstop level at f_1 is low attributes to low Q-factor of the discrete LC devices with a large inductance or capacitance value. The circuit simulation was accomplished by using Agilent ADS. Bias condition is V_{cc} = 6 V. As similar to the bandpass amplifier, 0.35 micron SiGe HBTs (Toshiba MT4S102T) with f_t = 25 GHz, chip inductors, capacitors, and resistors are employed in the simulation. The simulated bandstop frequencies in Fig. 5 are slightly lower than the target frequencies of 0.3, 0.5, 0.7, and 1 GHz. This is mainly due to the fact that the chip inductors, capacitors, and resistors include parasitic elements.

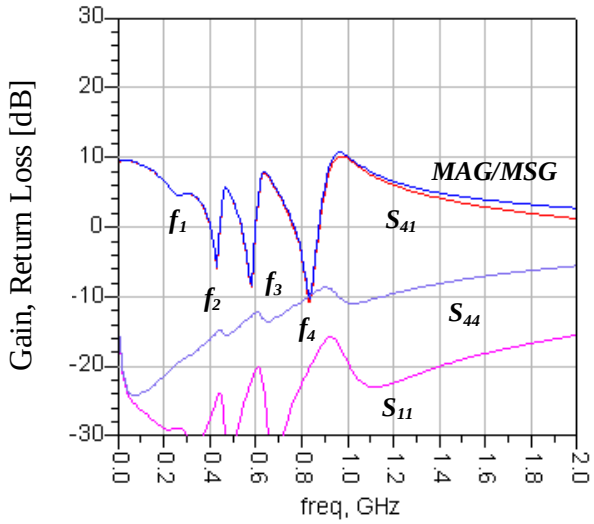

Fig. 5 Simulated results of the quad-band bandstop amplifier

4 Circuit Fabrication

A photograph of the quad-band bandpass and bandstop amplifiers is shown in Fig. 6. The amplifiers were fabricated on the FR-4 substrate with a dielectric constant of 4.5. 1005-type chip inductors, chip capacitors, chip resistors are mounted on the substrate by soldering. A surface mount type of the SiGe HBT (Toshiba MT4S102T) is used. The circuit size is 16 x 16 x 1.2 mm^3.

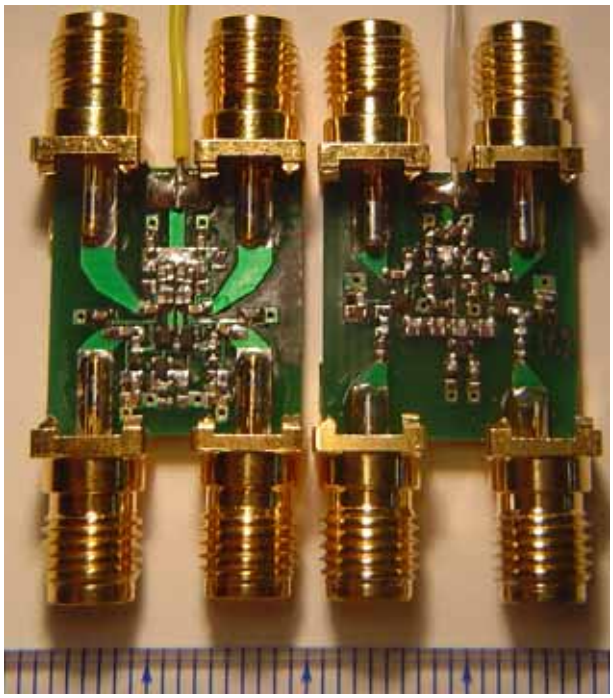

(a) Quad-band bandpass amplifier (b) Quad-band bandstop amplifier

Fig. 6 Photograph of the quad-band bandpass and bandstop amplifiers

5 Circuit Performance

5.1 Quad-Band Bandpass Amplifier

Measured gain and return loss of the quad-band bandpass amplifier are demonstrated in Fig. 7. The amplifier shows a gain of 7.3, 10.6, 9.1, and 10 dB at 0.54, 0.7, 1.08, and 1.39 GHz, respectively. The input and output return losses are better than 9 dB. Compared with the simulated results, the gain becomes lower and the matching frequency becomes higher especially for f_3 and f_4. The reason of

this discrepancy is discussed in the following chapter. Bias conditions are V_{CC} = 6 V and I_C = 21 mA.

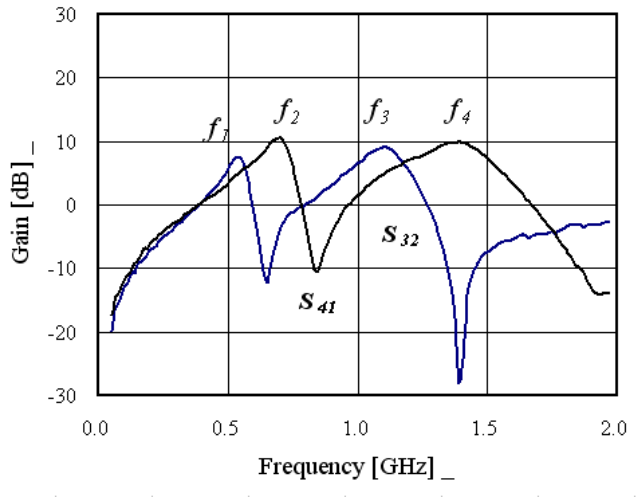

(a) Gain

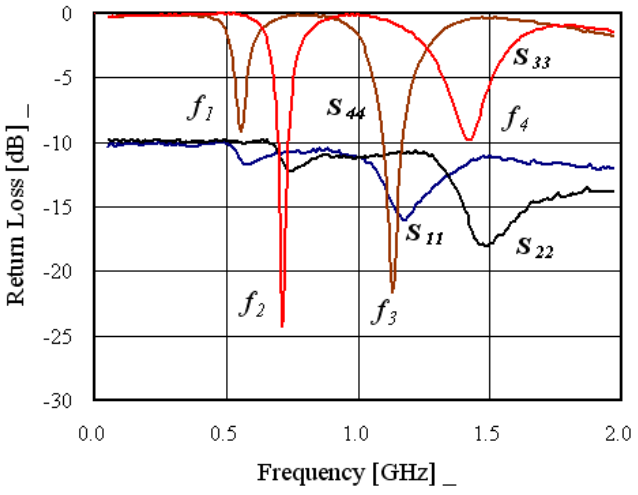

(b) Return loss

Fig. 7 Measured gain and return loss of the quad-band bandpass amplifier

5.2 Quad-Band Bandstop Amplifier

Measured gain, return loss, and isolation of the quad-band bandstop amplifier are shown in Fig. 8. The amplifier shows an averaged bandstop level of 6 dB at 0.34, 0.56, 0.73, and 1.07 GHz, respectively. The input and output return losses are better than 9 dB. Compared with the simulated results, the band rejection level becomes lower and the bandstop frequency becomes higher. The reason of this discrepancy is discussed in the following chapter. Bias conditions are V_{CC} = 6 V and I_C = 14 mA.

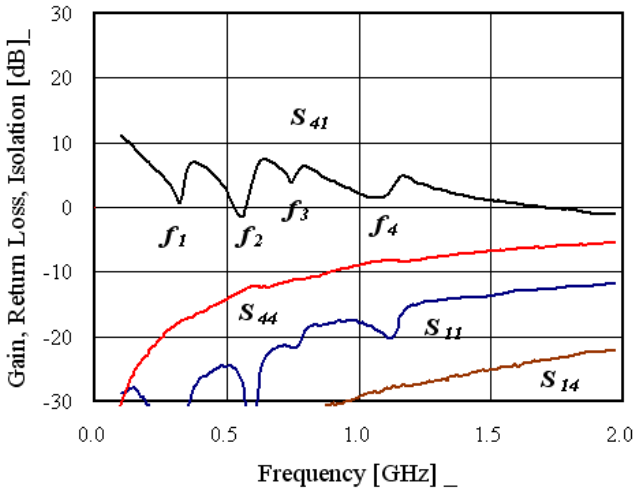

Fig. 8 Measured gain and return loss of the quad-band bandstop amplifier

6 Comparisons of Resonant Frequencies

In the previous chapter, a slight discrepancy appears between the simulated and measured bandpass or bandstop frequencies. To make clear the reason, the S-parameters of the parallel LC circuit with different values are simulated and measured. Table 1 shows the simulated and measured resonant frequencies (f_c) of the parallel LC circuits actually employed in the bandpass amplifier of Fig. 2. In Table 1, f_c is the calculated resonant frequency from Equation (2). It can be noted from Table 1 that the simulated and measured resonant frequencies of the parallel LC circuits as well as the simulated resonant frequency of the bandpass amplifier are in good agreement. The measured resonant frequency of the bandpass amplifier, however, becomes slightly higher. This is mainly due to the fact that the collector-to-emitter impedance of the differential transistor-pair adds to the stacked parallel-resonant circuits.

Table 1 Simulated and measured resonant frequencies of the parallel LC circuit and bandpass amplifier

No	1	2	3	4
L [nH]	1	1	1	1
C [pF]	82	39	28	10
fc [GHz]	0.56	0.81	1.19	1.59

fc of Parallel LC Circuit [GHz]				
Simulated	0.43	0.62	0.98	1.24
Measured	0.41	0.62	0.90	1.20
fc of Bandpass Amplifier [GHz]				
Simulated	0.43	0.63	0.97	1.22
Measured	0.54	0.70	1.08	1.39

Table 2 shows the simulated and measured resonant frequencies (f_c) of the parallel LC circuits actually employed in the bandstop amplifier of Fig. 4. In Table 2, f_c is the calculated resonant frequency from Equation (2). As similar to the bandpass amplifier, the simulated and measured resonant frequencies of the parallel LC circuits as well as the simulated resonant frequency of the bandpass amplifier are in good agreement. But the measured resonant frequency of the bandpass amplifier becomes slightly higher. The discrepancy is due to the fact that the current-source of the differential transistor-pair does not show ideally infinite impedance at microwave frequencies.

Table 2 Simulated and measured resonant frequencies of the parallel LC circuit and bandstop amplifier

No	1	2	3	4
L [nH]	1	1	1	1
C [pF]	220	82	47	22
fc [GHz]	0.34	0.56	0.73	1.07

fc of Parallel LC Circuit [GHz]				
Simulated	0.26	0.43	0.58	0.84
Measured	0.25	0.52	0.56	0.78
fc of Bandstop Amplifier [GHz]				
Simulated	0.26	0.43	0.58	0.84
Measured	0.33	0.55	0.72	1.07

7 Conclusions

L-band SiGe HBT differential amplifiers with multiple bandpass or bandstop performance have been presented. To achieve multiple bandpass or bandstop performance, multiple parallel-resonant circuits are cascaded in a stacked form and connected at the collector or between the emitters of the differential transistor-pair. With the use of the stacked parallel-resonant circuits, the quad-band bandpass amplifier demonstrates an averages gain of 9 dB at 0.54, 0.7, 1.08, and 1.39 GHz. Furthermore the quad-band bandstop amplifier shows an averaged bandstop level of 6 dB at 0.34, 0.56, 0.73, and 1.07 GHz. As for the bandpass or bandstop level, Q-factor of the stacked parallel-resonant circuit has to be improved. The multiple bandpass or bandstop technologies introduced in this paper would be one of the candidates supporting the current and future multiband, multimode, adaptive or reconfigurable wireless radios.

References

[1] E. McCune, High-efficiency, multi-mode, multi-band terminal power amplifiers, IEEE Microwave Magazine, 3 (2005), 44-55.

[2] S. Zhang, J. Madic, P. Bretchko, J. Mokoro, and R. Shumovich, A novel power-amplifier module for quad-band wireless handset applications, IEEE Trans. Microwave Theory & Tech., vol. 51, 11 (2003), 2203-2210.

[3] H. Nakajima and M. Muraguchi, Dual-frequency matching techniques and its application to an octave-band (30-60 GHz) MMIC amplifier, IEICE Trans. Electronics, vol. E80-C, 12 (1997), 1614-1621.

[4] Yu-Tso Lin and Shey-Shi Lu, A 2.4/3.5/4.9/5.2/5.7-GHz concurrent multiband low noise amplifier using InGaP/GaAs HBT Technology, IEEE Microwave and Wireless Component Letters, vol. 14, 10 (2004), 463-465.

[5] A. Raghavan, E. Gebara, M. Tentzeris, and J. Laskar, An active interference canceller for multi-standard collocated radio, IEEE MTT-S Digest, 6 (2005), 723-726.

[6] W. L. Chen, S. F. Chang, G. W. Huang, Y. S. Jean, and T. H. Yeh, A Ku-Band interference-rejection CMOS low-noise amplifier using current-reused stacked common-gate topology, IEEE Microwave and Wireless Component Letters, Vol. 17, 10 (2007), 718-720.

[7] T. K. Nguyen, N. J. Oh, C. Y. Cha, Y. H. Oh, G. J. Ihm, and S. G. Lee, Image-rejection CMOS low-noise amplifier design optimization techniques, IEEE Trans. MTT, Vol. 53, 2 (2005), 538-547.

Received: March 6, 2008